Pure Appl. Chem., Vol. 82, No. 1, pp. 149–159, 2010.
doi:10.1351/PAC-CON-09-01-06

Effect of aberrant disulfide bond formation on protein conformation and molecular property of recombinant therapeutics*

Lin Zhang, Murray Moo-Young, and C. Perry Chou‡

Department of Chemical Engineering, University of Waterloo, 200 University Avenue West, Waterloo, Ontario N2L 3G1, Canada

Abstract: As a comparative study, the extracytoplasmic domain of human CD83 (hCD83ext) was expressed as a glutathione-*S*-transferase (GST) fusion in two *Escherichia coli* B strains, i.e., BL21 and Origami B, respectively, with a reductive and oxidative cytoplasm. The final therapeutic products of hCD83ext produced by the two expression hosts exhibited significant differences in protein conformation and molecular property, which presumably resulted from different disulfide patterns. The study highlights the importance of developing proper host/vector systems and biomanufacturing conditions for the production of recombinant therapeutic proteins with a consistent product quality.

Keywords: disulfide bonds; *Escherichia coli*; gene expression; glutathione-*S*-transferase; human CD83; therapeutic proteins.

INTRODUCTION

Therapeutic proteins continue to play a pivotal role in human health care and the pharmaceutical industry. Approximately 150 therapeutic protein products with a current annual market value of US$ 50–60 billion have been commercialized, and at least 500 candidates are in various trial stages around the world [1]. While the use of mammalian expression systems for the production of therapeutic proteins has gained practical interest over the past decade, bacterium *Escherichia coli* retains its popularity as the workhorse primarily due to its well-characterized genome and mature techniques for genetic manipulation. Its importance is also reflected by the fact that 9 out of the 31 therapeutic proteins approved during 2003 and 2006 are produced in *E. coli* [1]. A critical issue associated with therapeutic protein production is the batch-to-batch consistency of product quality. Since therapeutic protein products often undergo an extensive storage before being clinically administered, their quality can be jeopardized by several protein deformation mechanisms, such as proteolysis, auto-degradation, misfolding, aggregation, oxidation, and other reactions, even under mild storage conditions.

Formation of aberrant disulfide bonds, either intra- or intermolecularly, has been recognized as a factor leading to undesired misfolding, multimerization, and subsequent loss of bioactivity for therapeutic proteins. Since disulfide bonds are formed by cross-linking cysteine pairs transiently close to each other, it is plausible to assume that the formation probability can be explicitly determined by protein structure or even intrinsically encoded by protein sequence. However, up to now, there is very limited knowledge and experimental demonstration as how protein conformation and/or protein sequence

*Paper based on a presentation at the 13th International Biotechnology Symposium (IBS 2008): "Biotechnology for the Sustainability of Human Society", 12–17 October 2008, Dalian, China. Other presentations are published in this issue, pp. 1–347.
‡Corresponding author: Tel.: 519-888-4567 ext. 33310; E-mail: cpchou@uwaterloo.ca.

can affect the formation mechanism associated with aberrant disulfide bonds. Theoretically, to ensure the consistent quality of therapeutic products, protein molecules should be designed and produced in such a way to both mediate a fixed disulfide pattern and to prevent the formation of aberrant disulfide bonds. In this regard, understanding various structural factors associated with disulfide bond formation becomes critical for quality production of therapeutic proteins at both the stages of molecular design and biomanufacturing.

Human CD83 (hCD83) is a 45 kDa glycoprotein on the membrane of dendritic cells. Structurally, mature hCD83 is composed of three domains, i.e., a cytoplasmic domain [39 amino acids (AAs)], a short transmembrane domain (22 AAs), and an extracellular Ig-like domain (125 AAs) (PDB accession number: Q01151). There are three sites (i.e., AAs 79, 96, and 117) for glycosylation and five cysteine residues (i.e., AAs 27, 35, 100, 107, and 129) involved in possible formation of inter- and intramolecular disulfide bonds. The immuno-related function for hCD83 is believed to lie in the extracellular domain since hCD83ext (i.e., hCD83 extracellular domain) could inhibit DC-mediated T cell stimulation [2] and was clinically effective in treating autoimmune disorder using the murine experimental autoimmune encephalomyelitis (EAE) model [3]. Structurally, hCD83ext can form a dimer via an intermolecular disulfide bond at Cys129 [4], and the biological activity of a Cys129Ser mutant variant has been evaluated [5].

Recently, we reported bioprocess development for the production of hCD83ext in *E. coli* [6]. However, the therapeutic product suffered inconsistent bioactivity, which could result from the formation of aberrant disulfide bonds in light of the observation of various hCD83ext monomeric and multimeric forms in product preparations [6]. Since hCD83ext was expressed as a glutathione-*S*-transferase (GST) fusion in the reducing cytoplasm of BL21, these aberrant disulfide bonds were supposed to be formed in vitro and rather randomly under oxidative conditions during downstream processing and product storage.

Theoretically, in vivo disulfide bond formation should be more consistent than in vitro formation since biological cells are able to maintain their intracellular environment rather steadily. In addition, intracellular disulfide bonds can be consistently processed by the Dsb-family members with rigorous formation mechanisms [7]. Though *E. coli* contains an oxidative periplasm in which disulfide bonds can be formed, heterologous protein expression targeting this compartment can be possibly limited by ineffective translocation. It is known that disulfide bond formation hardly occurs in the reductive cytoplasm of wild-type *E. coli*. However, the double mutation on the genes encoding thioredoxin reductase (*trxB*) and glutathione reductase (*gor*) [or glutathione synthetase (*gshB*)] can convert the reductive cytoplasm into an oxidative one, which offers an alternative expression compartment for proteins requiring disulfide bonds [8].

In this study, we used two *E. coli* B strains, i.e., BL21 and Origami B, respectively, with reductive and oxidative cytoplasm, to produce hCD83ext. With these two product preparations for parallel comparison, we demonstrated the significant effect of aberrant disulfide formation on protein conformation, which subsequently affected the molecular property of this therapeutic product.

MATERIALS AND METHODS

Bacterial strains and plasmids

The plasmid of pGEX2ThCD83ext containing the hCD83ext cDNA fused with the *gst* gene was used as the vector for expression of GST-hCD83ext under the regulation of an isopropyl β-D-thiogalactopyranoside (IPTG)-inducible *tac* promoter [9]. Due to the design of a thrombin cleavage site at the junction between GST and hCD83ext, the final hCD83ext product has four extra AAs, i.e., Gly-Ser-Pro-Gly, in the amino terminus and this modification was presumed to have no effect on the biochemical property of hCD83ext. BL21(DE3) and its *trxB* and *gor* double mutant derivative of Origami B(DE3) (EMD Biosciences/Novagen, La Jolla, CA, USA) were used as the expression host.

Cultivation and downstream processing

The production and purification of hCD83ext were conducted using the protocols developed previously [6]. In general, the *E. coli* production strain was cultivated in a bench-top bioreactor (Omni-Culture, VirTis, Gardiner, NY) containing 1-l working volume of culture medium [5 g/l NaCl, 20 g/l Bacto yeast extract, 20 g/l Bacto tryptone, 5 g/l glucose, and 10 µl/l Antifoam 289 (Sigma, St. Louis, MO, USA)]. The bioreactor was operated at pH 7.0, 28 °C, and 650 rpm, and was purged with filter-sterilized air at 2 l/min for aeration. When cell density reached ~2 OD_{600}, IPTG at 0.5 mM was added for induction and cells were harvested for downstream processing 6 h after induction. Cells were lysed and the cell lysate was loaded into a GST affinity chromatographic column (GE Healthcare, Baie d'Urfé, Québec, Canada). While binding to the GST affinity tags, GST-hCD83ext was subjected to on-column cleavage using thrombin to release the hCD83ext moiety, which was subsequently polished with anion exchange chromatography to remove endotoxin and other contaminant proteins. The fractions containing pure hCD83ext were pooled and concentrated with ultrafiltration using a high-pressurized stirred cell (Amicon, Model 8010 with YM10 disk, Millipore Canada, Cambridge, Ontario, Canada).

Sample treatment for analyses

The culture sample was appropriately diluted with saline solution for measuring cell density in OD_{600} with a spectrophotometer (DU®520, Beckman Coulter, Fullerton, CA, USA). For the preparation of cell extract, cells in the amount of 30 OD_{600}-units (defined as '$OD_{600} \times$ ml') were centrifuged at $6000 \times g$ and 2 °C for 10 min. The cell pellet was resuspended in 0.75 ml phosphate-buffered saline (pH 7.3), sonicated intermittently (i.e., 0.5 s/0.5 s on/off) for 4 min using an ultrasonic processor (Misonix, Farmingdale, NY, USA) with a microtip, and then centrifuged at $15\,000 \times g$ and 2 °C for 15 min to remove cell debris. The supernatant containing soluble proteins was used for various analyses, including GST assay, sodium dodecyl sulfate-polyacrylamide gel electrophoresis (SDS-PAGE), and Western blotting. The pellet containing insoluble proteins and cell debris was washed with phosphate buffer, resuspended in TE/SDS buffer (10 mM Tris HCl, pH 8.0, 1 mM EDTA, 1 % SDS), and heated to 100 °C for 5 min for dissolution. The protein content of the pellet was analyzed as the insoluble fraction.

Analytical methods

GST was assayed at ambient temperature using 1-chloro-2,4 dinitrobenzene (CDNB) and glutathione as the substrates. GST (or its fusion) catalyzes the reaction of the two substrates to form a conjugate product that can be monitored at 340 nm. One unit (U_{GST}) is defined as the amount of enzyme that causes an increase in absorbance at 1 OD_{340}/min. The protein concentration of purified hCD83ext was quantified with its absorbance at 280 nm (OD_{280}) and the extinction coefficient of 1.2 OD_{280}-ml/mg/cm. The number of titratable free sulfhydryl group was determined using the Ellman assay [10].

SDS-PAGE was performed in a Mini-PROTEAN®II electrophoresis cell (Bio-Rad) under both reducing and non-reducing conditions using a 12.5 % polyacrylamide separating gel stacked by a 4 % polyacrylamide stacking gel. Reduced and non-reduced protein samples were prepared using the 2X sample buffer respectively supplemented with 5 % 2-mercaptoethanol and 20 mM *N*-ethylmaleimide (NEM). Electrophoresis was conducted at a constant voltage of 200 V for approximately 45 min. The gel was stained with Coomassie blue or silver nitrate and dried. The dried gel was scanned. Compositions of monomer and dimer were quantified by measuring the pixels of their representing bands in the scanned gel images using UN-SCAN-IT software (Silk Scientific, Orem, UT, USA).

To conduct Western blotting, the proteins on the polyacrylamide gel were electroblotted to a poly(vinylidene difluoride) (PVDF) membrane after SDS-PAGE using a Mini Trans-Blot® Cell (Bio-Rad) according to a standard protocol [11]. The electrophoretic transfer was conducted at a constant

voltage of 100 V for 1 h. Protein-antibody hybridization was performed as described by Sambrook et al. [12]. The purified hCD83ext was used as an antigen for raising polyclonal anti-CD83 antibodies in rabbits. The secondary antibody was goat anti-rabbit IgG conjugated with horseradish peroxidase (Sigma). All hCD83-related polypeptides (e.g., GST-hCD83ext and hCD83ext) were detected by a colorimetric method using 3,3'-diaminobenzidine tetrahydrochloride (DAB) as the substrate. The processed membrane was scanned.

Far-UV circular dichroism (CD) spectra of protein samples were obtained using a spectropolarimeter (Jasco-815, Jasco, Japan). Fluorescence emission spectra (over the range of 300~420 nm) of protein samples were obtained using a spectrofluorometer (FP-6500, Jasco, Japan) with an excitation wavelength at 295 nm. All the spectroscopic measurements were conducted at ambient temperature of approximately 23 °C.

RESULTS

Bacterial cultivation for hCD83ext expression

Using BL21(DE3) and Origami B(DE3) as the host, cultivation for the expression of GST-hCD83ext was conducted in a bench-top bioreactor under identical operating conditions and the comparative results are summarized in Fig. 1. The growth rate of recombinant Origami B(DE3) was significantly lower than that of recombinant BL21(DE3), resulting in approximately 20 % reduction in both final cell density and specific GST activity (Figs. 1A,B). The reduction in growth rate for Origami strains was previously reported and attributed to possible malfunction of many cytoplasmic proteins under an oxidative condition [13]. However, the GST activity might not reflect the actual expression level of GST-hCD83ext since SDS-PAGE results indicated otherwise (Fig. 1C, lanes 2 vs. 4 and lanes 6 vs. 8) and this discrepancy appeared to be reproducible, suggesting that the oxidative environment in Origami B(DE3) could result in a certain level of reduction in GST activity.

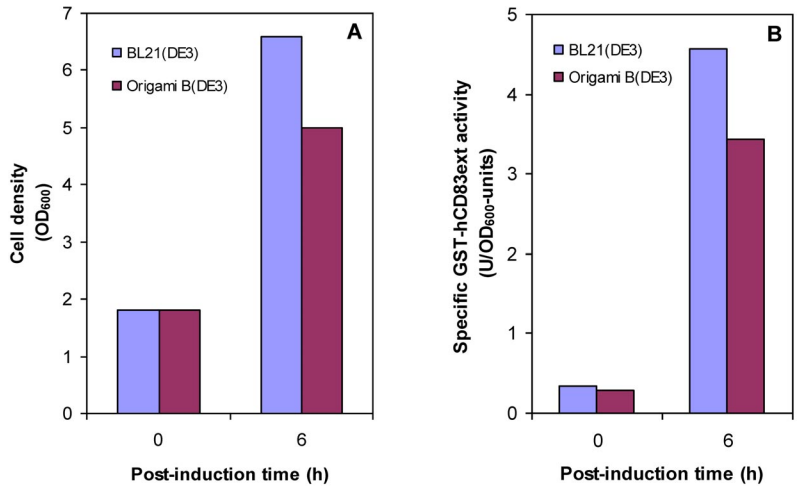

Fig. 1 Comparison of bioreactor cultivation performance for the production of GST-hCD83ext in two host strains: Cell density (panel A), specific GST activity (panel B), and intracellular protein analysis of both soluble and insoluble fractions under reducing and non-reducing conditions with SDS-PAGE (panels C) and Western blotting (panels D) for the culture samples taken prior to induction and at 6 h post-induction time are shown. Panel C: lanes 1, 2, 5, 6, 9 and 10 represent samples produced by BL21(DE3), whereas lanes 3, 4, 7, 8, 11, and 12 represent samples produced by Origami B(DE3). Arrows represent the protein bands corresponding to disulfided and non-disulfided hCD83ext monomers. Panel D: All lanes represent culture samples taken at 6 h post-induction time. Arrows represent the protein bands corresponding to various hCD83ext structures.

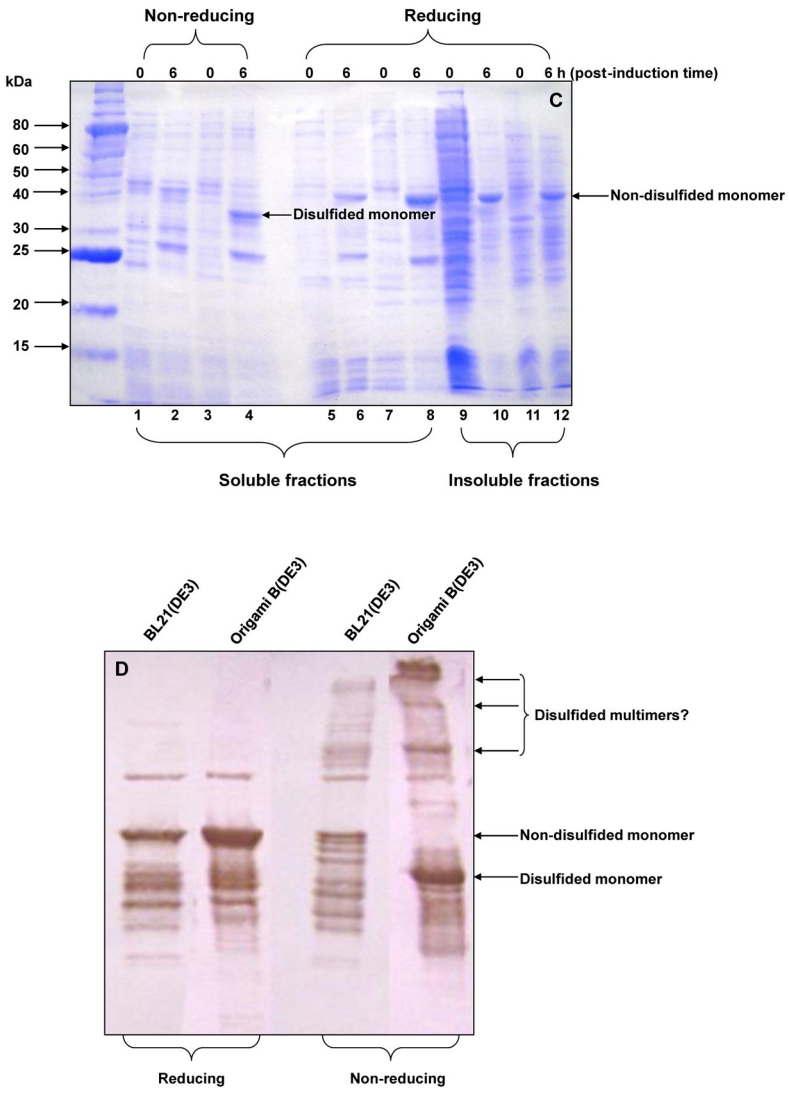

Fig. 1 (*Continued*).

Notice that, upon SDS-PAGE analysis, GST-hCD83ext expressed in Origami B(DE3) had a higher electrophoretic mobility under a non-reducing condition compared to that of its corresponding monomeric form under a reducing condition (Fig. 1C, lanes 4 vs. 8), indicating that certain intramolecular disulfide bond(s) formed in the oxidative cytoplasm. Unsurprisingly, such observation was not made when BL21(DE3) was used as the expression host since disulfide bonds cannot be formed in the reductive cytoplasm of wild-type *E. coli*. In addition, GST-hCD83ext expressed in both strains was not completely soluble though the expression in Origami B(DE3) was slightly more soluble than that in BL21(DE3) (Fig. 1C). Finally, it appeared that multimeric forms of GST-hCD83ext were produced via intermolecular disulfide bond(s) in Origami B(DE3) and these bands were verified to be associated with hCD83ext using Western blotting (Fig. 1D, lane 4).

Comparison of hCD83ext conformation

The expressed GST-hCD83ext from both production strains was trapped with GST-affinity chromatography and was subject to on-column cleavage with thrombin to release the hCD83ext moiety, which was then polished with anion exchange chromatography, concentrated, and formulated in 50 % glycerol for subsequent structural characterization. It appeared that the yield for the polishing step was moderately increased by in vivo disulfide bond formation (data not shown). Far-UV CD and fluorescent spectra of hCD83ext produced by the two strains were compared and the results are summarized in Fig. 2. Both hCD83ext samples displayed a CD spectrum with a negative band at 220 nm and a positive band near 203 nm (Fig. 2A), which is a typical pattern for β-sheets mixed with type II β-turns [14]. The spectrum of hCD83ext produced by BL21(DE3) had a lower band at 203 nm and a deeper trough at 220 nm, compared to that of hCD83ext produced by Origami B(DE3). Based on the spectroscopic simulation using the K2D method [15], the two hCD83ext preparations had slightly different compositions in the secondary structure, i.e., the ratio of α-helix: β-sheet: unordered structure at 9, 43, 48 % for hCD83ext produced by BL21(DE3) and 4, 48, 48 % for hCD83ext produced by Origami B(DE3).

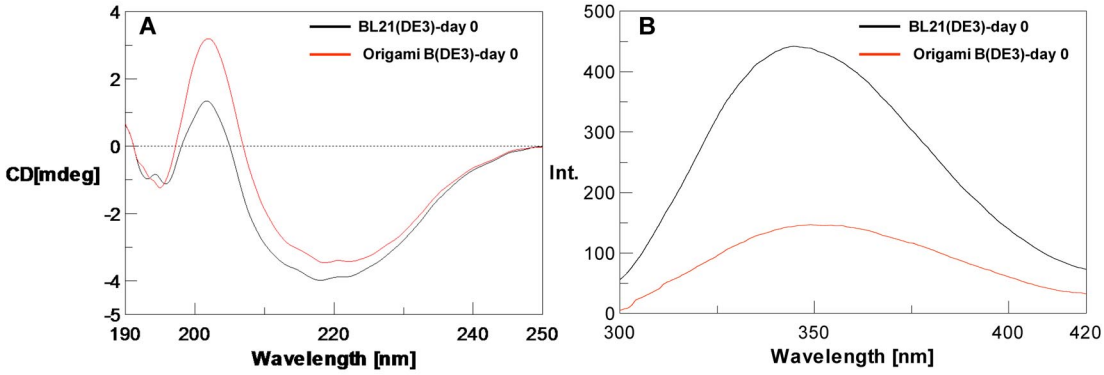

Fig. 2 Analysis of protein structure for fresh hCD83ext produced by two host strains with CD spectroscopy (panel A) and fluorescence spectroscopy (panel B).

Since hCD83ext has two tryptophan residues (i.e., AAs 39 and 49), the emission spectrum reflecting the local environment near the tryptophan residues can shed light on the tertiary structure. The maximum emission intensity (at 345 nm) of hCD83ext produced by BL21(DE3) was approximately 3-fold that (at 350 nm) of hCD83ext produced by Origami B(DE3) with a slight red-shift (Fig. 2B), implying significantly different 3D conformation for the two protein preparations.

Given significant conformational differences between the two hCD83ext variants, the SDS-PAGE analysis however revealed a rather similar pattern (lane 2 in Figs. 3A~D) except the observation that hCD83ext produced by BL21(DE3) had two monomeric forms (lane 2, Fig. 3C) whereas hCD83ext produced by Origami B(DE3) only had a single monomeric form (lane 2, Fig. 3D). On the other hand, the number of titratable free sulfhydryl group was 0.96 and 0.63 under a native condition for hCD83ext produced by BL21(DE3) and Origami B(DE3), respectively (Figs. 4A,B).

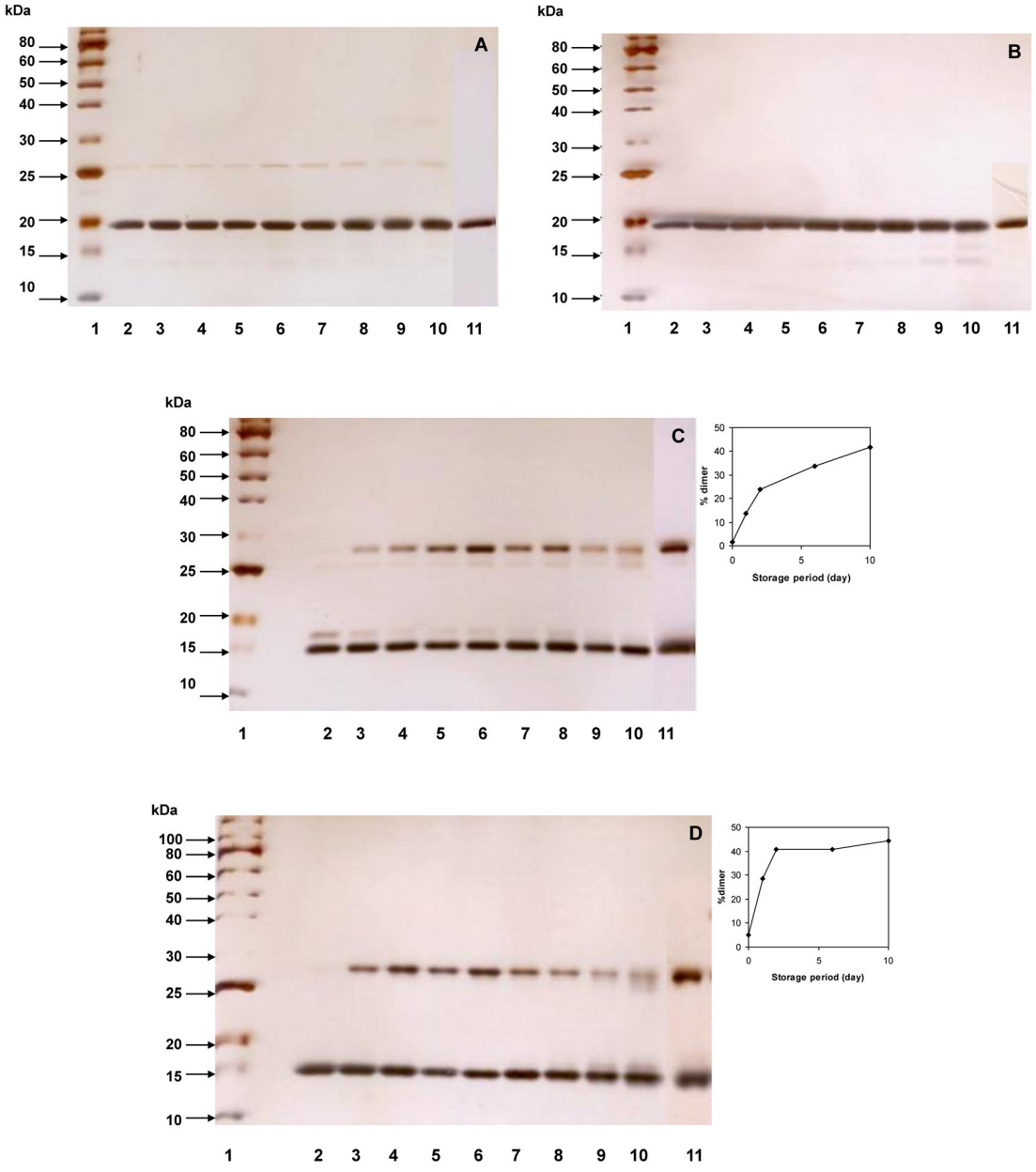

Fig. 3 Monitoring and comparison of molecular property for hCD83ext produced by two host strains with reducing SDS-PAGE (panels A and B), non-reducing SDS-PAGE (panels C and D), CD spectroscopy (panels E and F), and fluorescence spectroscopy (panels G and H): Samples up to 30-day storage at –20 °C and 10-day storage at room temperature were analyzed. Panels A, C, E, and G represent hCD83ext samples produced by BL21(DE3), whereas panels B, D, F, and H represent hCD83ext samples produced by Origami B(DE3). Panels A~D: lane 1/molecular weight markers; lane 2/day 0; lanes 3~6 and 11/–20 °C samples taken on days 1, 2, 6, 10, and 30, respectively; lanes 7~10/room temperature samples taken on days 1, 2, 6, and 10, respectively. The insets at upper right in panels C and D represent the time profiles for dimerization of hCD83ext stored at –20 °C. Such quantification was not conducted for samples stored at room temperature since hCD83ext dimer appeared to be unstable.

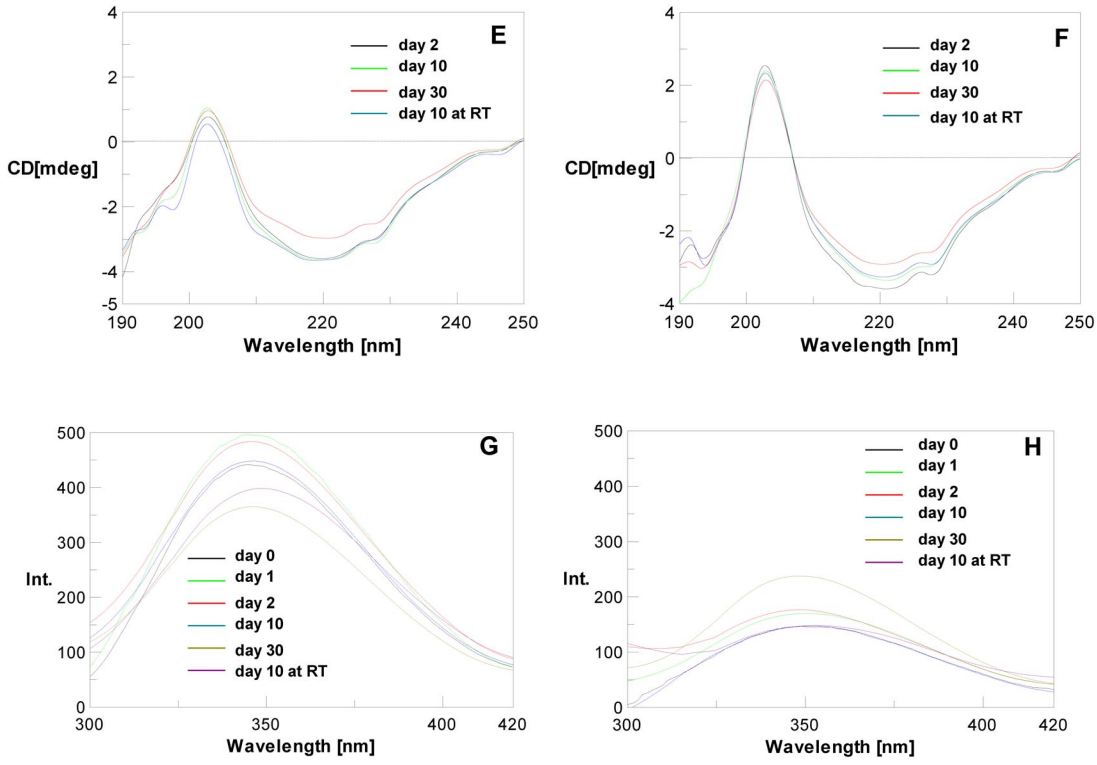

Fig. 3 (*Continued*).

Comparison of hCD83ext molecular property

The molecular property of the two hCD83ext variants was compared by monitoring the conformational changes under storage conditions (either –20 °C or room temperature) and the results are summarized in Figs. 3 and 4. While the two protein samples had an identical band pattern upon reducing SDS-PAGE (Figs. 3A,B), two rather different dimerization profiles over the incubation period were observed upon non-reducing SDS-PAGE, particularly for the samples stored at –20 °C (Figs. 3C,D). Compared to hCD83ext produced by BL21(DE3), hCD83ext produced by Origami B(DE3) appeared to have a higher tendency for initial dimerization. The monomeric doublet corresponding to hCD83ext produced by BL21(DE3) disappeared over the storage period. The rate of dimerization for hCD83ext appeared to increase noticeably when incubated at room temperature, particularly for hCD83ext produced by BL21(DE3). Notice that, while the hCD83ext monomers corresponding to the two protein samples were rather stable at room temperature, the dimers started to degrade after 2 days of incubation (Figs. 3C,D, lanes 8–10).

The far-UV CD spectra with respect to storage time suggest that both hCD83ext variants did not experience significant changes in the secondary structure (Figs. 3E,F) during the storage, even in the presence of dimerization and dimer degradation. Results of fluorescence spectra revealed a slight red-shift upon 10 days of incubation at room temperature, presumably associated with dimer degradation (Figs. 3G,H). The maximum intensity of emission spectrum for hCD83ext produced by BL21(DE3) monotonically decreased with incubation time; whereas that for hCD83ext produced by Origami B(DE3) appeared to fluctuated with a significant increase for the 30-day sample stored at –20 °C. The decreasing trend in the number of titratable free sulfhydryl group suggests that disulfide bonds were

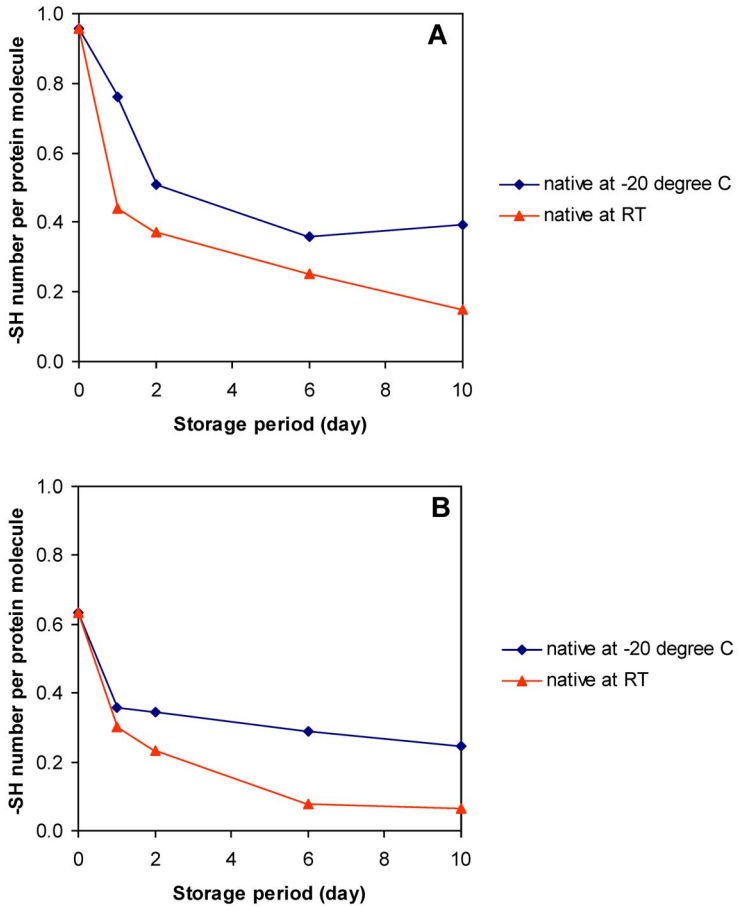

Fig. 4 Time profiles for the number of titratable free sulfhydryl group in hCD83ext produced by BL21(DE3) (panel A) and Origami B(DE3) (panel B): Profiles for samples stored at –20 °C and room temperature are shown.

continuously being formed (Fig. 4). Overall, the above results suggest the conformational changes in the tertiary structure over the storage period.

DISCUSSION

There are five cysteine residues in hCD83ext, and it was reported that hCD83ext can form dimers in vitro via a major intermolecular disulfide bond at Cys129 [4]. However, in vivo disulfide bond formation within GST-hCD83ext at the protein expression level was not previously explored. The present results show that GST-hCD83ext fusion contained no disulfide bonds when expressed in the reductive cytoplasm of BL21(DE3), but contained intramolecular or even intermolecular disulfide bond(s) when expressed in the oxidative cytoplasm of Origami B(DE3). The Cys27 residue in the hCD83ext moiety could play a key role for such in vivo disulfide bond formation since no monomer with a higher electrophoretic mobility was observed for the GST fused with the Cys27 mutant derivative of hCD83ext expressed in Origami B(DE3) (manuscript in preparation). Though the precise location(s) of such in vivo disulfide bond formation was not characterized, the protein conformation and molecular property of the final hCD83ext product were significantly affected by this post-translational processing at the protein expression level.

With respect to the protein conformation, it appeared that the two hCD83ext variants had rather distinct secondary structures (based on CD spectra) and tertiary structures (based on fluorescent spectra) though SDS-PAGE revealed a very similar pattern. Since the expression host was the only difference in the "Materials and methods" section upon producing these two variants, it is plausible to assume that the structural differences could result from different disulfide patterns, namely, hCD83ext produced by Origami B(DE3) might contain an extra unconventional intramolecular disulfide bond(s) bridged in vivo. Analysis of hCD83ext sequence reveals an immunoglobulin (Ig) domain with a conserved disulfide bond between Cys35 and Cys107. In addition, our prediction of 3D structure (data not shown) also suggests Cys27 and Cys100 are spatially close enough to form a possible disulfide bond. However, the argument cannot be verified by reducing SDS-PAGE since the major monomeric bands for both variants had approximately the same electrophoretic mobility (Figs. 3C,D). Interestingly, an extra monomeric band with a lower electrophoretic mobility was observed in day-0 sample for hCD83ext produced by BL21(DE3) and we speculated that it could represent un-disulfided hCD83ext. If this argument were true, the major monomeric band for hCD83ext produced by BL21(DE3) would also contain a disulfide bond(s), which were presumably formed in vitro and rather effectively during downstream processing normally conducted in an oxidative environment. To address these technical issues, characterization of disulfide pattern for hCD83ext variants using mass spectroscopy is currently under extensive exploration in our lab.

The presence of the extra intramolecular disulfide bond(s) for hCD83ext produced by Origami B(DE3) mediated a slight shift in the composition of the secondary structure of hCD83ext from α-helix to β-sheet with a minimum influence on the composition of the unordered structure. While the local environment surrounding the two tryptophan residues in the two hCD83ext product variants appeared to be similar in terms of tryptophan exposure ($\lambda_{max} > 340$ nm), the emission fluorescence was slightly red-shifted ($\Delta\lambda_{max} = 5$ nm; implying a more polar local environment surrounding the two tryptophan residues) and significantly quenched for hCD83ext produced by Origami B(DE3). Emission quenching via disulfide bonds which acted as electron scavengers absorbing electrons from excited indole ring of tryptophan was previously reported [16]. Alternatively, the hCD83ext variant with an intramolecular disulfide bond(s) could possibly develop a conformation that facilitates the transfer of emission energy, resulting in the above quenching. Apparently, these conformational changes potentially associated with intramolecular disulfide bond formation enhanced the subsequent formation of intermolecular disulfide bond for dimerization, possibly by shifting the local environment and orientation of cysteine residues to facilitate their spatial contact. The results indirectly suggest that transient protein structure or even protein sequence likely correlate with the probability of having cysteine residues to appear within a contact range to form aberrant disulfide bonds.

It was previously reported that hCD83ext should be stored under frozen conditions due to its intrinsic instability [6]. Though protein degradation was prevented at –20 °C, hCD83ext tended to form dimers or even multimers via intermolecular disulfide bonds [6]. The present results show that the rate of dimerization increased with temperature. In addition, both monomers and dimers were rather stable at –20 °C, whereas dimers were less stable than monomers at room temperature. Apparently, prolonged incubation of hCD83ext at a relatively high temperature resulted in faster dimerization and subsequent degradation, which could be a major cause for the intrinsic instability. Nevertheless, the stability issue appeared to be unaffected by the presence of unconventional disulfide bonds.

ACKNOWLEDGMENTS

This work was supported by the Natural Sciences and Engineering Research Council (NSERC), and the Canada Research Chair (CRC) program of Canada. We are grateful to A. DeAraujo (NPS-Allelix) for contributing lab supplies and W. Yao for offering lab assistance.

REFERENCES

1. G. Walsh. *Nat. Biotechnol.* **24**, 769 (2006).
2. M. Lechmann, D. Krooshoop, D. Dudziak, E. Kremmer, C. Kuhnt, C. G. Figdor, G. Schuler, A. Steinkasserer. *J. Exp. Med.* **194**, 1813 (2001).
3. E. Zinser, M. Lechmann, A. Golka, M. B. Lutz, A. Steinkasserer. *J. Exp. Med.* **200**, 345 (2004).
4. M. Lechmann, N. Kotzor, E. Zinser, A. T. Prechtel, H. Sticht, A. Steinkasserer. *Biochem. Biophys. Res. Commun.* **329**, 132 (2005).
5. E. Zinser, M. Lechmann, A. Golka, B. Hock, A. Steinkasserer. *Immunobiol.* **211**, 449 (2006).
6. Y. Xu, L. Zhang, W. Yao, S. S. Yedahalli, S. Brand, M. Moo-Young, C. P. Chou. *Protein Expr. Purif.* **65**, 92 (2009).
7. J. Messens, J. F. Collet. *Int. J. Biochem. Cell Biol.* **38**, 1050 (2006).
8. P. S. Stewart. *Biotechnol. Bioeng.* **59**, 261 (1998).
9. M. Lechmann, E. Kremmer, H. Sticht, A. Steinkasserer. *Protein Expr. Purif.* **24**, 445 (2002).
10. N. Darby, T. E. Creighton. *Mol. Biotechnol.* **7**, 57 (1997).
11. H. Towbin, T. Staehelin, J. Gordon. *Proc. Natl. Acad. Sci. USA* **76**, 4350 (1979).
12. J. Sambrook, E. F. Fritsch, T. Maniatis. *Molecular Cloning: A Laboratory Manual*, Cold Spring Harbor Laboratory Press, New York (1989).
13. P. H. Bessette, F. Aslund, J. Beckwith, G. Georgiou. *Proc. Natl. Acad. Sci. USA* **96**, 13703 (1999).
14. N. Sreerama, R. W. Woody. In *Circular Dichroism: Principles and Applications*, N. Berova, K. Nakanishi, R. W. Woody (Eds.), pp. 601–620, John Wiley, New York (2000).
15. M. A. Andrade, P. Chacon, J. J. Merelo, F. Moran. *Protein Eng.* **6**, 383 (1993).
16. A. Holmgren. *J. Biol. Chem.* **247**, 1992 (1972).

